

# Study on the Influence of Length-to-Depth-Ratio on the Flow Characteristics of High-Speed Cavities

Pengcheng Cui<sup>1,2</sup>, Jie Zhang<sup>1,\*</sup>, Yueyue Yang<sup>1</sup>, Hongyang Chen<sup>1</sup>, Tao Mo<sup>1</sup>,  
Liang Liu<sup>1</sup>, Chuan Jia<sup>1</sup>, Long Wu<sup>1</sup>, Yingying Shen<sup>1</sup>, Guiyu Zhou<sup>1,\*</sup>

<sup>1</sup> Computational Aerodynamics Institute, China Aerodynamics Research and Development Center,  
Mianyang, 621000, China

<sup>2</sup> State Key Laboratory of Aerodynamics, China Aerodynamics Research and Development Center,  
Mianyang, 621000, China

\*Corresponding author e-mail: pccui@foxmail.com

**Abstract.** With the improvement of China's economic level and the increasing diversification of cultural consumption demand, the anime and manga industry has become an important part of the cultural industry. Enterprises generate income through the development of derivatives or collect rights fees as a source of profit through the licensing of cartoon images. Under the background of new media, cartoon characters display various personality characteristics of cartoon images through cross-media platforms such as the Internet, gain the emotional recognition of consumers, and then promote the sales and development of animation derivatives. Based on the theory of customer perceived value, this paper puts forward the research on the marketing strategy of animation derivatives.

**Keywords:** Animation Derivatives; Customer Perceived Value, New Media Communication.

## 1. Introduction

In recent years, in order to meet the requirements of drag reduction, stealth, and supersonic cruise, most new aircraft have adopted embedded cavities, such as B-2 and F-22. Due to the removal of external weapon mounting brackets and hangers, the radar reflection area of the buried bomb compartment has been significantly reduced, while also reducing the aerodynamic resistance and thermal effects caused by external weapon mounting. However, when the weapon bay is opened and the cavity is exposed to free high-speed flow, there exists complex unsteady flows inside the cavity, including shock wave flow interference, boundary layer separation, shear layer interference and vortex motion, directly affecting the structural safety of the aircraft and the safe separation of missiles. Therefore, it is very necessary to conduct research on the flow characteristics of cavities.

The Length-to-Depth-Ratio ( $L/D$ ) is a very important dimensionless parameter for cavities. As the  $L/D$  increases, the flow characteristics of the cavity will significantly change, and some researchers have conducted detailed research on the flow characteristics of cavities. Yang studied the effect of geometry parameters of length to depth ratio and width to depth ratio on cavity flow pattern and noise characteristics in low speed[1]. Yan studied the effects of Mach number, length to depth ratio of activity and separation distance from activity on longitudinal aerodynamic characteristics of a general store in personal activity flow based on numerical method[2]. Sridhar invested in the unsteady flow in a two dimensional rectangular open cell with emphasis on the effects of length to depth ratio on the shear layer development and cell drag based on numerical simulations and experiments[3]. Cui studied the flow characteristics and acoustic characteristics in a  $L/D=6$  at subsonic speed and found the pressure distribution in such activity may lead to the head up attribute of the store[4]. Li experimentally invested in the flame stabilization with cavity strut injection of ethylene in a single side expansion scramjet combiner[5].

However, most previous studies are focused on subsonic, transonic, and low supersonic speeds, with limited research on the flow characteristics of cavities at higher speeds, and the range of  $L/D$  is usually only 5-10. On the basis of previous studies, this paper studies the flow characteristics of higher Mach numbers and wider  $L/D$  ranges, laying the foundation for the research of advanced aircraft.

## 2. Numerical Method

The simulations in this paper are conducted by the China Aerodynamics Research & Development Center (CARD C) NNW-FlowStar flow solver[6], which is a large-scale general computational fluid dynamics (CFD) numerical simulation software developed independently by the project team with the support of the National Numerical Wind Tunnel Engineering for aircraft aerodynamic calculation and analysis in the aerospace field[7].

### 2.1 Governing Equations

This paper takes the Reynolds averaged Navier Stokes equation (RANS) in integral form as the governing equation. For three-dimensional steady compressible flow, the conservative form of the NS equation can be written as:

$$\frac{\partial}{\partial \tau} \iiint_V \mathbf{W} dV + \iint_{\Omega} (\mathbf{F}_c - \mathbf{F}_v) dS = 0 \quad (1)$$

Where,  $\mathbf{W} = [\rho \quad \rho u \quad \rho v \quad \rho w \quad \rho E]^T$ , and the fluxes can be described as:

$$\mathbf{F}_c = \begin{bmatrix} \rho V \\ \rho u V + p n_x \\ \rho v V + p n_y \\ \rho w V + p n_z \\ \rho H V \end{bmatrix}, \quad \mathbf{F}_v = \begin{bmatrix} 0 \\ n_x \tau_{xx} + n_y \tau_{xy} + n_z \tau_{xz} \\ n_x \tau_{yx} + n_y \tau_{yy} + n_z \tau_{yz} \\ n_x \tau_{zx} + n_y \tau_{zy} + n_z \tau_{zz} \\ n_x \Theta_x + n_y \Theta_y + n_z \Theta_z \end{bmatrix} \quad (2)$$

### 2.2 Geometry and Computational meshes

Fig.1 shows the cavity model studied in this paper, similar to the M219 standard model, this model has a large flat plate underneath the cavity. The length of the cavity is 4m and the width is 1m. This paper adjusts L/D by adjusting the depth of the cavity, while keeping the length and width of the cavity unchanged during the research. This paper sets a wide range of aspect ratios from 3 to 16. Fig.2 shows the computational mesh of this paper, which adopts a mixed grid. Hexahedral and triangular prismatic grids are used as much as possible near the cavity wall to better simulate viscosity. Tetrahedral and pyramid mixed grids are used for the far field, and grids are appropriately encrypted near the wall. Spatial grid refinement is carried out in areas where the shear layer of the cavity may go through, the total grid amount of the mesh is 13.72 million.

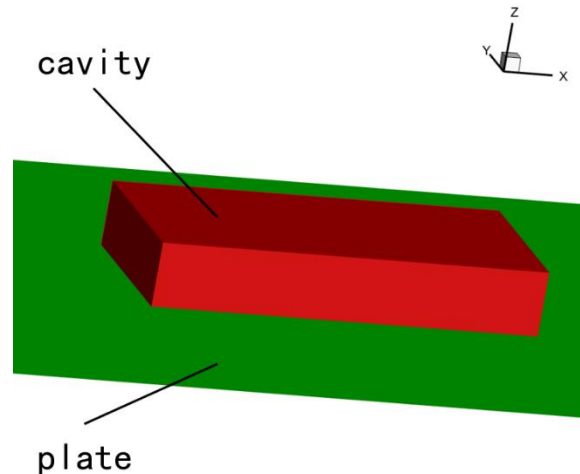
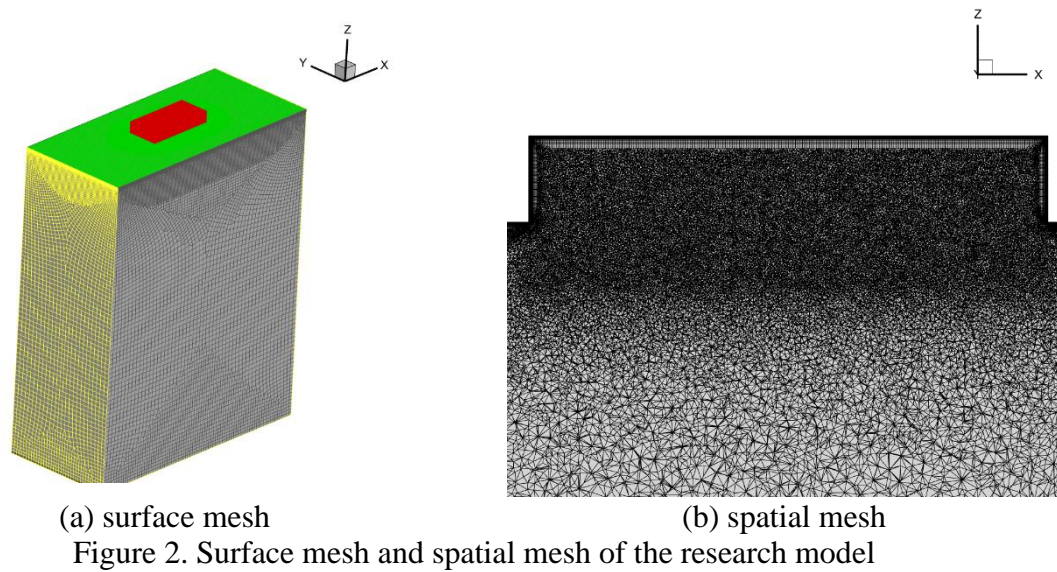


Figure 1. The cavity model in this paper.



### 2.3 Validation of numerical method

M219 cavity is a benchmark model designed by the European DESider project, which has full and accurate wind tunnel data and is often applied to validate the cell flow predictions [8-10]. Fig.3 shows the size of M219 cavity, and the length to depth ratio is 5.

Fig.4 shows the comparison of the flow characteristics and acoustic characteristics of CFD and experiment results. The results show that the numerical results in this paper are qualitatively and quantitatively comparable to the wind tunnel.

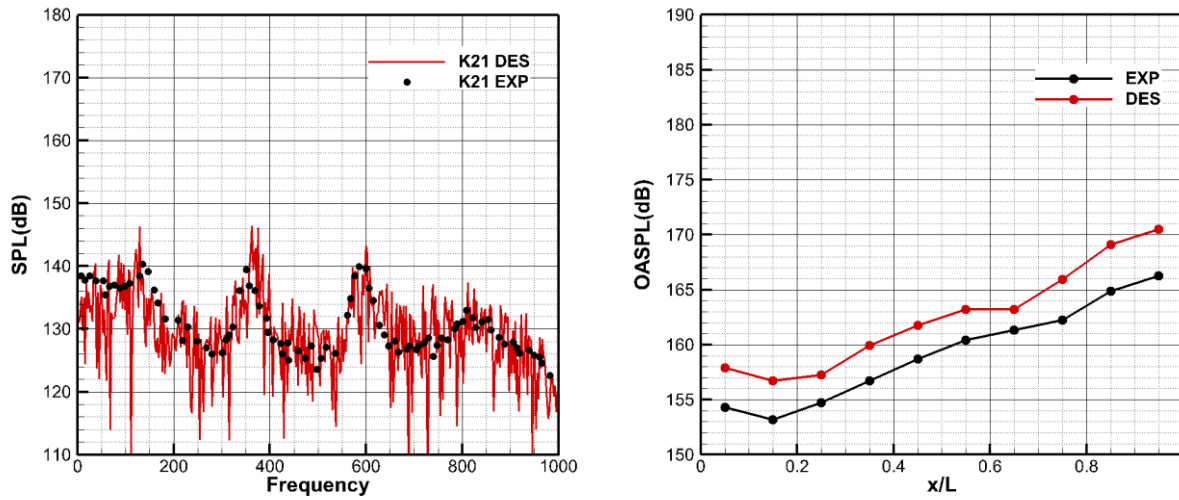


Figure 4. Comparison of with experiment

### 3. Results and Discussion

#### 3.1 The flow characteristics of typical $L/D$

Fig. 5 shows the spatial Mach number distribution and pressure gradient contour of the cavity when the  $L/D$  is 6 with an incoming Mach number of 2. It can be seen that the cavity presents a typical characteristic of an open cavity. Due to the small  $L/D$ , the shear layer directly crosses the entire cavity, collides with the rear of the cavity, and forms local high pressure. The leading edge of the cavity forms an expansion wave due to the expansion of the flow towards the interior of the cavity, while the trailing edge of the cavity forms a strong shock wave due to the rapid convergence and compression of flow.

Fig. 6 shows the spatial Mach number distribution and pressure gradient contour surface of a cavity with an aspect ratio of 10 with an incoming Mach number of 2.0. It can be seen that the cavity presents a typical characteristic of a transitional cavity, where the shear layer of the cavity collides with the bottom of the cavity in the middle and forms a strong compression shock wave. At the same time, there are expansion waves and shock waves at the leading and trailing edges of the cavity, respectively.

Fig. 7 shows the spatial Mach number distribution and pressure gradient contour surface of a cavity with an aspect ratio of 16 with an incoming Mach number of 2.0. It can be seen that the cavity presents a typical characteristic of a closed cavity. The airflow separates at the leading edge of the cavity and expands into the cavity, reaching the bottom of the cavity to form an impact shock wave. Afterwards, the airflow adheres to the bottom of the cavity. Before reaching the rear wall of the cavity, the airflow separates again and expands outward, forming an overflow shock wave. The impact shock wave and overflow shock wave will merge into one shock wave outside the cavity.

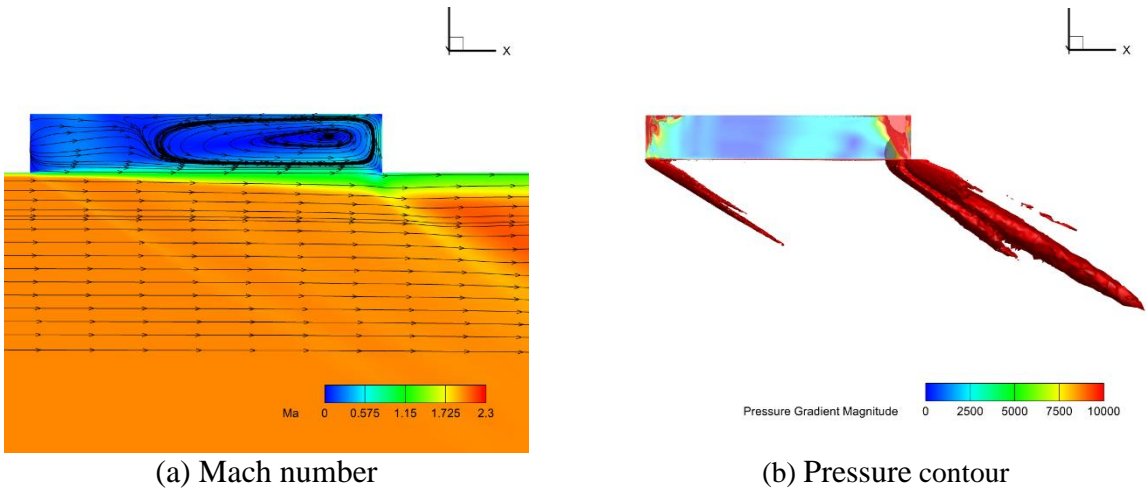


Figure 5. The flow characteristics of  $L/D=6$

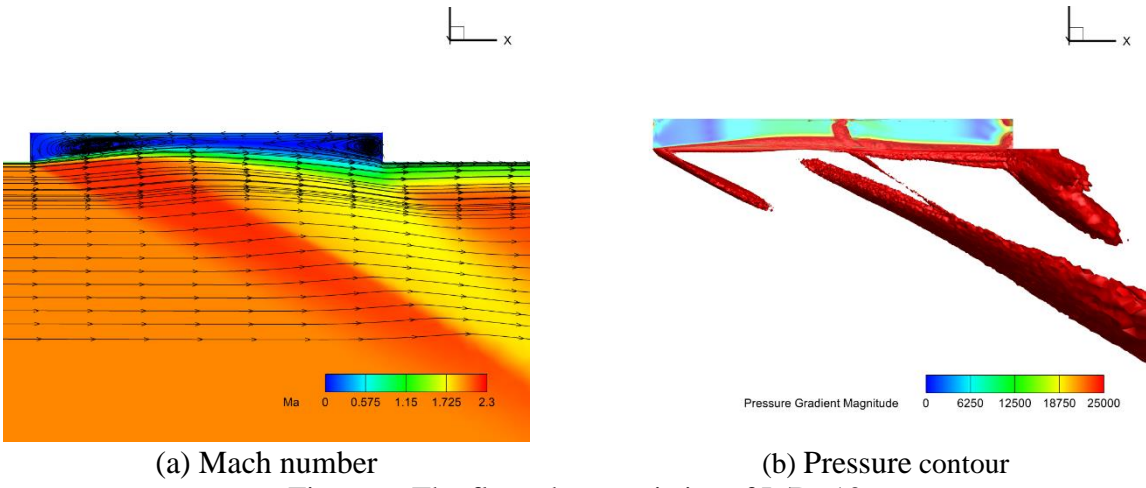


Figure 6. The flow characteristics of  $L/D=10$

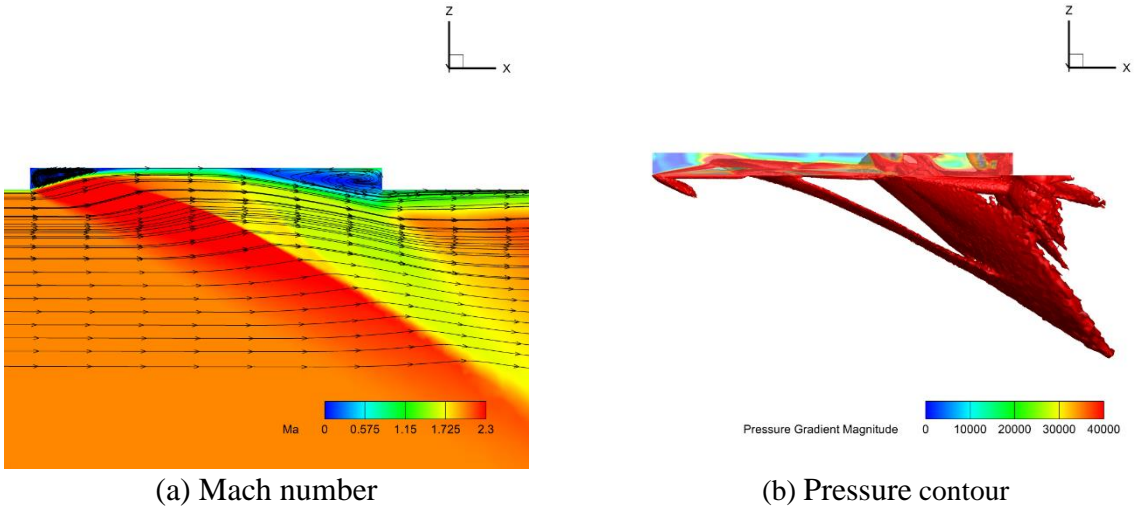


Figure 7. The flow characteristics of  $L/D=16$



### 3.2 Flow characteristics from low-speed to high-speed

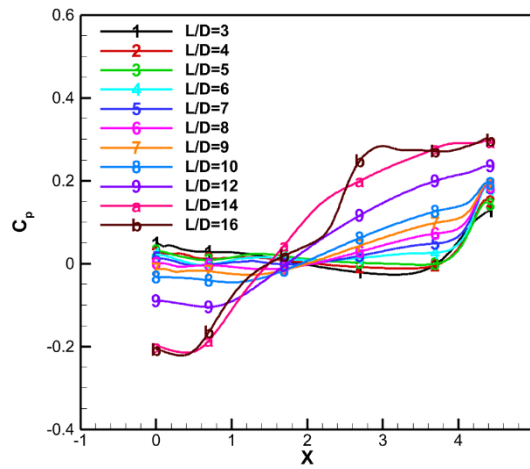


Figure 8. Pressure distribution at Ma =2.

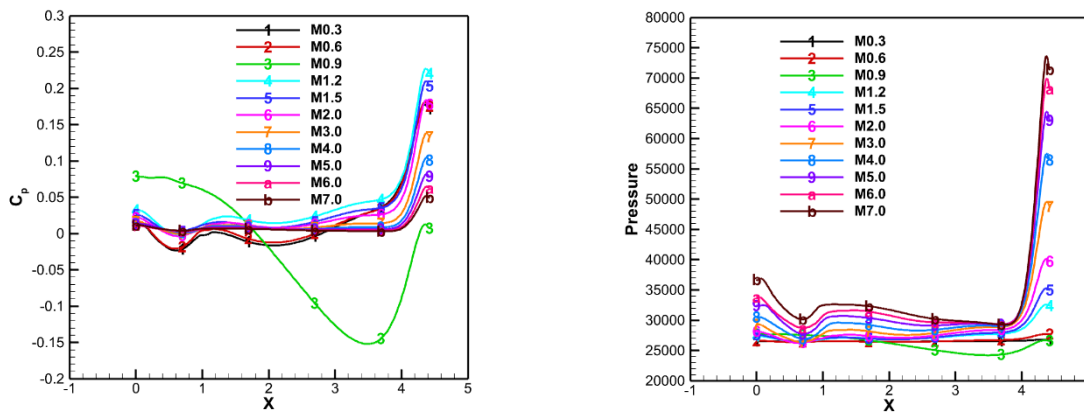


Figure 9. Pressure distribution of the cavity with L/D=6.0

Figure 8 shows the pressure distribution at the bottom of the cavity for different L/D at Mach number=2. When the L/D is large, the cavity is a closed flow, and in this case, the typical pressure distribution at the bottom of the cavity is: the expansion zone behind the front wall of the cavity is low-pressure, and the pressure increases near the impact cavity. The attachment zone of the flow corresponds to a pressure platform. When the flow approaches the back wall of the cavity and separates and forms an overflow shock wave, the pressure rises again and reaches its maximum value before the back wall of the cavity. When the L/D decreases, the flow field in the cavity changes from closed flow to transitional flow. At this time, the shear layer rotates at an angle at the leading edge of the cavity, and the flow collides with the bottom of the cavity while leaving the cavity, causing the impact shock wave and overflow shock wave to merge into one shock wave inside the cavity. When corresponding to the flow type, the longitudinal pressure at the bottom of the cabin monotonically increases from the low value behind the front wall to the maximum value in front of the rear wall. At this time, the pressure platform corresponding to the attachment zone of the closed flow airflow disappears. As the L/D further decreases, the flow field in the cavity begins to transition from transitional flow to open flow. At this time, the flow in the rear wall area of the cavity is completely connected to the flow in the front wall area of the cavity, forming a large vortex inside the cavity. The incoming flow forms a shear layer at the front edge of the cavity and directly crosses over the cavity. The pressure coefficient on the bottom surface of the entire cavity is relatively uniform, basically maintaining a small positive value. However, there is a large pressure gradient near the rear

wall of the cavity, which is caused by the compression of the flow caused by the impact of the shear layer on the outer edge of the rear wall of the cavity.

Figure 9 shows the pressure distribution at the bottom of the cavity with an  $L/D$  of 6.0, where all cavity flows are open flow. This is a very typical  $L/D$  ratio in engineering practice, indicating that open flow should be very common in engineering applications. However, the ideal cavity configuration in this article is very simple, with no components loaded inside the cavity. There may be complex configurations in actual engineering, and further research is needed.

## 4. Conclusion

This paper investigates the influence of the  $L/D$  of a cavity on flow characteristics. The  $L/D$  ranges from 3 to 16, and the velocity ranges from subsonic to hypersonic. The results show that at the same Mach number, as the  $L/D$  increases, the cavity flow gradually transitions from open to closed. Under supersonic conditions, closed and transitional cavities will form high pressure at the rear of the cavity, which is unfavorable for the store separation. In common aircraft cavities, the pure cavity is usually an open flow, while in engineering practice, the internal structure of the cavity is complex and requires further detailed research.

## Acknowledgments

This work was financially supported by National Natural Sciences Foundation of China (12102453) and National Numerical Wind Tunnel (NNW).

## References

- [1] Yang G, Sun J, Liang Y, et al. Effect of geometry parameters on low speed cavity flow by wind tunnel experience [J] AASRI Procedia, 2014, 9:44-50.
- [2] Yan P P, Zhang Q F, Li J. Numerical study of strong interplay between cavity and store during launch [J] Journal of Mechanics, 2018, 34 (2): 103-112.
- [3] Sridhar V, Gai S L, Kleins H. Oscillatory characteristics of shallow open cavities in personal flow [J] AIAA Journal, 2016, 54 (11): 3495-3508.
- [4] Cui P, Zhou G, Zhang Y, et al. Improved Delayed Detached Eddy Investments on the Flow Control of the Leading Edge Flat Spoiler of the Capacity in the Low Aspect Ratio Aircraft [J] Aerospace, 2022, 9 (9): 526.
- [5] Li F, Sun M, Cai Z, et al. Experimental study of flame stabilization in a single side expansion scramjet combiner with different cavity length to depth ratios [J] Acta Astronautica, 2020, 173:1-8.
- [6] Cui P, Jia H, Chen J, et al. Numerical investigation on unsteady shock wave/vortex/turbulent boundary layer interactions of a hypersonic vehicle during its shroud separation[J]. Aerospace, 2022, 9(10): 619.
- [7] Cui P, Zheng Y, Xu P, et al. The comparison of adjoint-based grid adaptation and feature-based grid adaptation method[C]//Journal of Physics: Conference Series. IOP Publishing, 2022, 2280(1): 012003.
- [8] L. Temmerman, B. Tartinville, C. Hirsch. URANS Investigation of the Transonic M219 Cavity[J]. Springer Berlin Heidelberg, 2012.
- [9] S Lawson, G N Barakos, P Nayyar, et al. Appendix for M219 cavity flow: Computations with and without bay doors. 2009.
- [10] Y P X, B J Q, G B Z, et al. Suppression Effect of Jet Flow on Aerodynamic Noise of 3D Cavity[J]. Applied Mechanics and Materials, 2014, 444-445(5):588-595.